BIOCHEMISTRY

ATP as a biological hydrotrope

Avinash Patel,[1]* Liliana Malinovska,[1]* Shambaditya Saha,[1] Jie Wang,[1] Simon Alberti,[1] Yamuna Krishnan,[2]† Anthony A. Hyman[1]†

Hydrotropes are small molecules that solubilize hydrophobic molecules in aqueous solutions. Typically, hydrotropes are amphiphilic molecules and differ from classical surfactants in that they have low cooperativity of aggregation and work at molar concentrations. Here, we show that adenosine triphosphate (ATP) has properties of a biological hydrotrope. It can both prevent the formation of and dissolve previously formed protein aggregates. This chemical property is manifested at physiological concentrations between 5 and 10 millimolar. Therefore, in addition to being an energy source for biological reactions, for which micromolar concentrations are sufficient, we propose that millimolar concentrations of ATP may act to keep proteins soluble. This may in part explain why ATP is maintained in such high concentrations in cells.

Many biological compartments form by liquid-liquid phase separation, and the viscosity of these compartments is known to be dependent on adenosine triphosphate (ATP) (*1*–*3*). To investigate this phenomenon further, we tested the effect of ATP on the formation of liquid compartments formed by purified fused in sarcoma (FUS). In healthy cells, FUS forms liquid compartments that are involved in transcription, DNA repair, and RNA biogenesis (*4*–*7*). We reconstituted FUS compartments in vitro at physiological concentration (*7*) using low salt (70 mM) buffer conditions (*8*) and tested the effect of ATP around its physiological concentration range of 2 to 8 mM (*9*), complexed with Mg^{2+} ions (ATP-Mg) (*10*). (For the chemical structures of all compounds used in this paper, see figs. S1A and S2A.) Indeed, 8 mM ATP-Mg prevented liquid-liquid phase separation and dissolved previously formed drops (Fig. 1, A and B). We observed similar effects of ATP with other proteins that form liquid compartments (*11*) (Fig. 1, A and B). A fluorescent tracer molecule confirmed that ATP was enriched in the liquid drops (Fig. 1C). Importantly, APPNP was as efficient as ATP in preventing the formation of liquid drops (Fig. 1, D and F). Thus, at millimolar concentrations, ATP dissolved drops independently of its role as an energy source.

Changing the ionic strength of a solution can strongly influence electrostatic interactions by changing the Debye screening length. This might drive a phase separation known as the salt effect (*12*, *13*) (see the supplementary materials for details on salt effect). However, increasing the amount of salt (KCl) to physiologically relevant concentrations (150 mM) showed a negligible effect on phase separation of FUS (Fig. 1, D and E, and fig. S1, B to D). This observation was consistent with salts of different valences, and only solutions with an ionic strength above physiologically relevant concentration were able to perturb phase separation (Fig. 1E and fig. S1, B and C).

We investigated whether other physiologically relevant, structurally related nucleotides could affect FUS phase separation. Guanosine triphosphate (GTP) dissolved drops with a concentration similar to that of ATP (fig. S1E). Both adenosine diphosphate (ADP) and adenosine monophosphate (AMP) dissolved drops, but at higher concentrations than ATP (fig. S1F). Because the intracellular concentrations of ADP, AMP, and GTP are ~200, ~200 to 800, and ~400 μM (*9*, *14*), respectively, they would have negligible effects in vivo on the solubilization of liquid compartments. TP-Mg had a negligible effect on FUS drop dissolution (Fig. 1, D to F, and fig. S1, B and C), indicating that the charge density in the ionic ATP side chain alone is insufficient for the dissolution of FUS drops. Taken together, our data show that the tripolyphosphate moiety combined with the adenosine confers a chemical property to ATP that is manifested at millimolar concentrations.

The hydrophilic tripolyphosphate moiety and a relatively hydrophobic adenosine ring provide ATP with an amphiphilic property. Several amphiphilic small molecules, such as sodium xylene sulfonate (NaXS) or sodium toluene sulfonate (NaTO), function as hydrotropes and are commonly used in industrial processes to solubilize hydrophobic compounds (*15*–*18*). First described by Neuberg in 1916, hydrotropes are a class of amphiphilic, organic small molecules that increase the solubility of sparingly soluble organic molecules in water by several orders of magnitude (*16*, *17*). Hydrotrope action seems to involve a preferential nonstoichiometric accumulation of hydrotrope molecules around the solute. In addition, their aggregation is dependent on the presence of solute molecules, and they do not adopt any well-defined superstructure on their own, unlike surfactants (*19*–*21*). Given the similarities between classical hydrotropes and ATP (Fig. 2A), we sought to explore whether ATP might act like a hydrotrope in a classical hydrotrope assay, in which the solubility of a hydrophobic compound such as fluorescein diacetate (FDA) in water is quantified as a function of hydrotrope concentration (*15*). For a hydrotrope such as NaXS, as its concentration increases, FDA solubility in water increases and the latter is quantified by ultraviolet absorption at 480 nm of the aqueous medium (Fig. 2B, upper panel). NaXS required concentrations greater than ~1 M to effectively solubilize FDA (Fig. 2B). However, ATP achieved the same effect at concentrations as low as 100 mM (Fig. 2B, lower panel). Water-soluble assemblies comprising amphiphiles (e.g., hydrotropes and surfactants) (fig. S2A) structured around a hydrophobic molecule consist of relatively nonpolar interior microenvironment. An organic dye, ANS (8-anilino-1-naphthalenesulfonic acid) is commonly used to probe the polarity near the head group (hydrophilic) or interfacial region of such amphiphilic assemblies. The fluorescence emission maximum of ANS is blue-shifted in a hydrophobic microenvironment (Fig. 2C, upper panel). Thus, the concentration at which the blue shift of ANS is maximal is a widely used indicator of the effectiveness of a hydrotrope (*15*, *22*). Classical hydrotropes such as NaXS and NaTO induce a blue shift in the emission spectrum of ANS (*15*). ATP altered the emission spectrum of ANS to the same degree as NaXS and NaTO, albeit at much lower concentrations (Fig. 2C, lower panel). This shows that ATP is much more efficient than classical hydrotropes for creating a solubilizing microenvironment for hydrophobic molecules that are unlike micelles (fig. S2B and supplementary text). Furthermore, we found that similar to ATP, NaXS can dissolve FUS liquid drops (Fig. 2, D and E). The solubilization of proteins in cells has also been attributed to osmolytes inside a cell (*23*, *24*). However typical osmolytes could not recapitulate the effect of ATP on FUS droplet solubilization (fig. S2, A and C, and supplementary text).

We next investigated whether high concentrations of ATP could also prevent protein aggregation. Using a centrifugation assay, we showed that millimolar concentrations of ATP kept FUS soluble and that higher concentrations of ATP prevent FUS aggregation (Fig. 3, A and B, and fig. S3, A to C). Notably, millimolar concentrations of ATP could also dissolve preformed FUS fibers, albeit at higher concentrations than were required to prevent aggregation (Fig. 3, C and D, and fig. S3, D to F). We also showed, using incorporation of thioflavin T, that ATP prevents the aggregation of two proteins that tend to cause amyloids: (i) synthetic Aß42 peptides, which aggregate to form Amyloid beta, associated with Alzheimer's disease (*25*); and (ii) the prion domain of the yeast protein Mot3 (Mot3-PrD), which is thought to form functional aggregates in yeast cells (*26*) (Fig. 3, E and F).

To investigate the role of ATP in a more physiological mixture of biological molecules at physiological concentrations, we studied protein aggregation in chicken egg white. At high

[1]Max Planck Institute of Molecular Cell Biology and Genetics, 01307 Dresden, Germany. [2]Department of Chemistry and Grossman Institute for Neuroscience, Quantitative Biology, and Human Behavior, University of Chicago, Chicago, IL 60637, USA.
*These authors contributed equally to this work. †Corresponding author. Email: yamuna@uchicago.edu (Y.K.); hyman@mpi-cbg.de (A.A.H.)

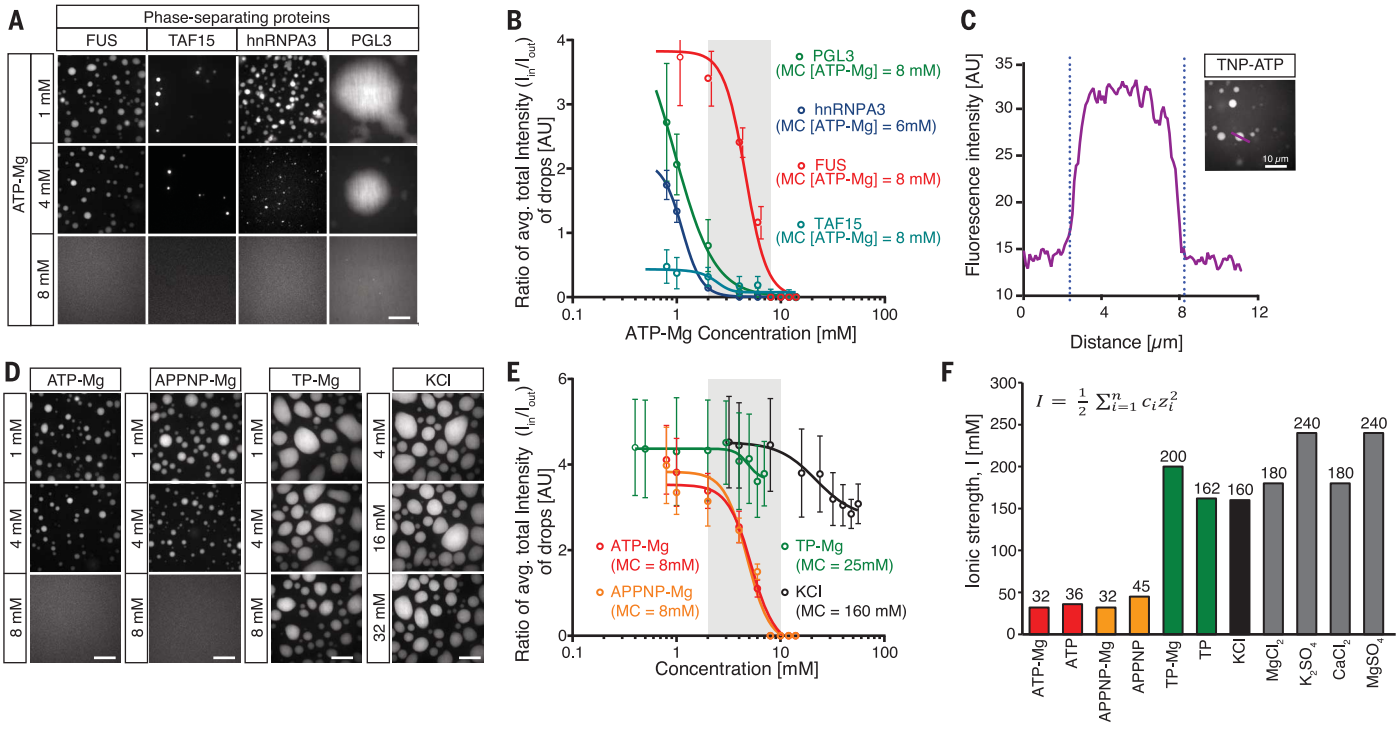

Fig. 1. ATP inhibits the phase separation of unstructured proteins. (**A**) Fluorescent images of phase-separated protein drops treated with ATP-Mg at different concentrations. FUS-GFP was used at 5 μM, TAF15-Snap-Alexa Fluor 546 was used at 1 μM, hnRNPA3-GFP was used at 25 μM, and PGL-3-GFP was used at 2.5 μM. Phase-separated drops formed in low-salt buffer (70 mM). Increasing concentration of ATP-Mg inhibited phase separation. Scale bar, 10 μm. (**B**) Quantification of phase separation. FUS-GFP, TAF15-Snap-Alexa Fluor 546, hnRNPA3-GFP, and PGL-3-GFP were used at 7 μM, 1 μM, 25 μM, and 2.5 μM, respectively. Phase separation is determined as the ratio of protein inside drops (I_{in}) to protein outside drops (I_{out}). Total fluorescence intensity of protein is taken as a measure for protein amount. Decreasing I_{in}/I_{out} ratios reflect inhibition of phase separation. Lines represent fitted dose-response curves [log(concentration) versus I_{in}/I_{out} ratio]. MC[ATP-Mg] is the minimal concentration of ATP-Mg needed to inhibit phase separation. Error bars, mean ± SD (N = 36). The physiological concentration range of ATP-Mg is highlighted in gray. (**C**) ATP enrichment inside the phase-separated FUS droplet phase. 2,4,6-trinitrophenol-ATP (ATP-TNP) (1 μM) was used as fluorescent tracer for ATP in a solution of phase-separated FUS protein. Line scan of fluorescent intensity of ATP-TNP (plotted across the magenta line) indicates fourfold enrichment inside the droplet phase compared with the surrounding solution. (**D**) Fluorescent images of phase-separated FUS-GFP protein drops treated with ATP-Mg, APPNP-Mg, salt (KCl), and magnesium tripolyphosphate (Mg-TP). FUS-GFP was used at 5 μM. The range of concentrations of all added reagents was adjusted to match the range of ionic strength of ATP-Mg (see the supplementary materials for details). Phase separation is inhibited by 8 mM of ATP-Mg and APPNP-Mg. Scale, bar 10 μm. (**E**) Quantification of phase separation [conditions as in (D)] with FUS-GFP used at 7 μM. MC is the minimal concentration needed to inhibit phase separation. Error bars, mean ± SD (N = 36). (**F**) Quantification of minimum ionic strength needed to disrupt phase separation of FUS-GFP in the presence of different reagents. FUS-GFP was used at 7 μM. Ionic strength was calculated using the shown equation, where c is concentration, z is the charge of the ion, and n is the number of ions in a solution (see the supplementary materials for details).

temperatures, egg proteins lose their native conformation, thus exposing hidden hydrophobic patches within the proteins, which drive the aggregation of egg-white proteins. ATP inhibited the aggregation of boiled egg white in a dose-dependent manner (Fig. 4, A to C; fig. S4, A and B; and movie S1). Thus, ATP appears to prevent aggregation of egg white by stabilizing the native globular state (fig. S4C).

Taken together, our experiments suggest that ATP has two different chemical properties. At micromolar concentrations, it acts as an energy source to drive chemical reactions, whereas at millimolar concentrations it acts to solubilize proteins.

The action of ATP at millimolar concentrations to solubilize proteins is reminiscent of the known activity of a hydrotrope. Since their description by Neuberg (*16*), hydrotropes have been widely employed in industry to achieve highly concentrated aqueous formulations of hydrophobic compounds. They modify viscosity and cloud point, minimize phase separation at ambient temperatures, and reduce foaming. They reduce long-range ordering of amphiphilic or hydrophobic molecules by forming a stacked, highly dynamic layer around the solute molecules to produce a continuous isotropic solution (*15*). The data showing that the hydrophobic adenosine ring of ATP strongly enhances the effect of the charged tripolyphosphate moiety on protein stability are consistent with the hypothesis that ATP also acts as a hydrotrope, where the aromatic group could form dynamic clusters around hydrophobic solute molecules (*17*, *19*, *21*). However, the precise molecular mechanism underlying the action of ATP to stabilize biological molecules remains to be elucidated (*23*, *27*–*30*). Recently, rigorous statistical thermodynamic theories indicate that it is the preferential nonstoichiometric binding/clustering of hydrotrope molecules around a solute that could explain molecular mechanisms behind hydrotrope action (*19*–*21*). ATP might be a suitable biological hydrotrope because of interactions of both its charged and hydrophobic moieties with the amino acids of proteins.

The high concentration of ATP in cells has long been a puzzle, because ATP-dependent enzymes require micromolar concentrations of ATP. Why, then, would a cell invest so much energy into maintaining its cytoplasmic ATP concentration at ~5 mM? One explanation is that the free-energy difference between ATP and ADP is required to drive ATP-dependent reactions and that the

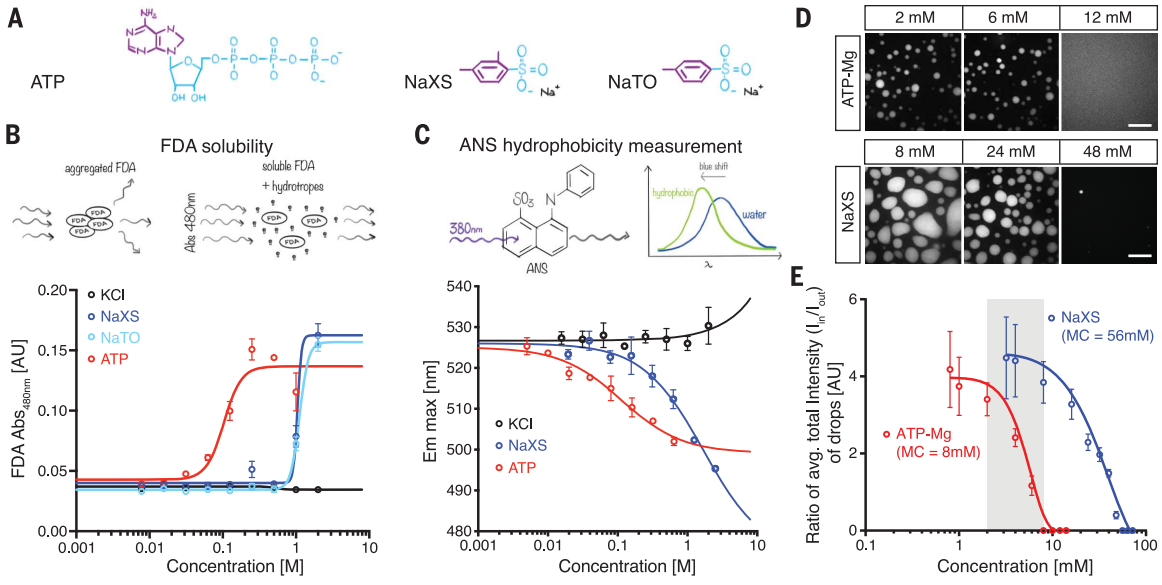

Fig. 2. Hydrotrope-like properties of ATP. (**A**) Comparison of chemical structure of ATP, NaXS, and NaTO. The molecules have a hydrophobic aromatic ring (purple) and a short hydrophilic, charged residue (blue). (**B**) Effect of ATP-Mg, NaXS, NaTO, and salt on the solubility of FDA in aqueous solutions at room temperature as measured by the absorbance at 480 nm. If in solution, FDA absorbs light at 480 nm, while aggregated FDA scatters light (schematics). Lines represent fitted dose-response curves [log(concentration) versus absorption of FDA at 480 nm]. Error bars, mean ± SD (*N* = 3). (**C**) ATP-Mg solutions offer a less polar environment than water. The variation of the fluorescence spectral band maximum of the probe ANS is shown as a function of the concentration of ATP-Mg and NaXS. ATP-Mg solutions exhibit the most prominent blue shift. Lines represent fitted dose-response curves [log(concentration) versus emission maxima of ANS]. Error bars, mean ± SD (*N* = 3). (**D**) Fluorescent images of phase-separated FUS-GFP protein drops treated with ATP-Mg and NaXS. FUS-GFP was used at 5 μm. Scale bar, 10 μm. (**E**) Quantification of phase separation [conditions as in (D)] with FUS-GFP used at 7 μm. The range of concentrations of NaXS was adjusted to match the range of ionic strength of ATP-Mg (see the supplementary materials for details). MC is the minimal concentration needed to inhibit phase separation. Error bars, mean ± SD (*N* = 36).

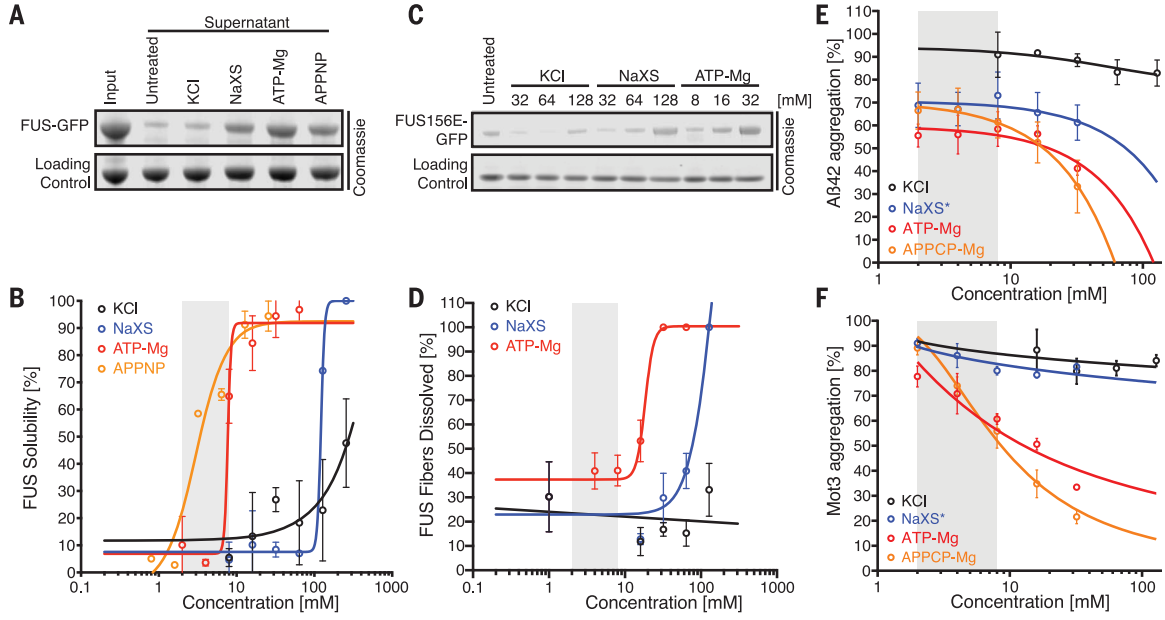

Fig. 3. Inhibition of protein aggregation by hydrotropes. (**A**) Hydrotropes enhance the solubility of FUS-GFP. FUS-GFP (input) at high concentration (40 μM) had a limited solubility in low-salt buffer conditions (150 mM) after cleavage of the tagged solubilizing domain [maltose binding protein (MBP)]. Soluble FUS-GFP in the supernatant after centrifugation of aggregated FUS-GFP was visualized on a SDS–polyacrylamide gel electrophoresis (SDS-PAGE) gel stained with Coomassie blue. ATP-Mg and its nonhydrolysable analog, APPNP, enhanced the solubility of FUS-GFP to a similar extent as NaXS. Cleaved MBP tag served as the loading control. (**B**) Dose-response curve of FUS-GFP solubility in the presence of ATP-Mg, APPNP, and NaXS. Lines represent fitted dose-response curves [log(concentration) versus soluble fraction with respect to total input of FUS-GFP]. Error bars, mean ± SD (*N* = 3). (**C**) ATP dissolves preformed FUS aggregates. Mutant FUSG156E-GFP (5 μM) was aged to induce aggregation. Hydrotropes were added after aggregate formation and incubated for 12 hours. Soluble fractions were visualized on a SDS-PAGE stained with Coomassie blue. ATP and NaXS dissolve the FUS aggregates at high concentrations (32 mM and 128 mM, respectively). Lysozyme was spiked into the assay as a loading control. (**D**) Quantification of the solubilization of FUS aggregates [conditions as in (C)]. Lines represent fitted dose-response curves [log(concentration) versus soluble fraction with respect to total input of FUS-GFP]. Error bars, mean ± SD (*N* = 3). (**E** and **F**) ATP-Mg prevents fiber formation. Thioflavin T (ThT) was incorporated in amyloid fibers and displays an enhanced fluorescence (Ex 440nm/Em 480nm). ATP-Mg or nonhydrolysable APPCP-Mg prevented formation of amyloid fibers of Aß42 peptide (E) and the prion domain of the yeast Mot3 protein (Mot3-PrD) (F) in a concentration-dependent manner. Lines represent fitted dose-response curves [log(concentration) versus aggregated protein assessed by ThT emission]. Error bars, mean ± SD (*N* = 3). The range of concentrations of all added reagents was adjusted to match the range of ionic strength of ATP-Mg (see the supplementary materials for details).

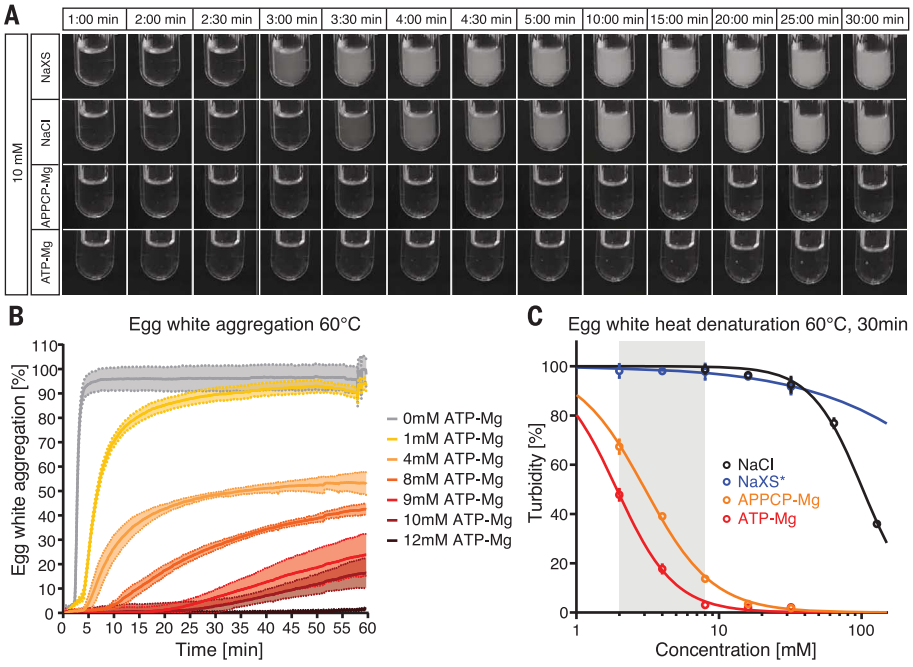

Fig. 4. ATP enhances protein stability. (**A**) Heat denaturation of crude egg white can be inhibited by addition of ATP-Mg. Crude egg white was heated at 60°C in a water bath in the presence of equimolar (10 mM) amounts of ATP-Mg, nonhydrolysable APPCP-Mg, and NaXS. NaCl (40 mM) was used to match the ionic strength of ATP-Mg. Over 30 min, the aggregation of egg white is abolished in the presence of ATP-Mg and APPCP-Mg. (**B**) The stabilization of heat-denatured egg white is concentration dependent. The kinetic traces of egg-white aggregation [conditions as in (A)] in the presence of increasing concentrations of ATP-Mg over 60 min. The amount of egg-white aggregation is assessed by changes of the pixel value (integrated density). Four mM of ATP-Mg blocked aggregation by 50%, whereas 12 mM of ATP-Mg completely abolished aggregation. The shaded area represents the range of the standard error (n = 3). (**C**) The dose response for stabilization of heat-denatured egg white. The amount of egg-white aggregation was assessed by turbidity measurement in a 96-well plate. The aggregation of egg white decreases with increasing concentrations. Lines represent fitted dose-response curves [log(concentration versus aggregated material assessed by turbidity measurement]. Error bars, mean ± SD (N = 3). The range of concentrations of all added reagents was adjusted to match the range of ionic strength of ATP-Mg (see the supplementary materials for details).

50-fold higher ATP/ADP ratio is necessary to fuel the myriad metabolic reactions taking place simultaneously in a cell. However, cytoplasm can have protein concentrations over 100 mg/mL (*31*–*33*), and it is extremely difficult to maintain such high protein concentrations in a test tube without spontaneous aggregation. The hydrotrope activity of ATP may help keep proteins soluble in the cytoplasm (*34*) and provide another, but not mutually exclusive, explanation for high ATP concentrations in cells. Possibly also, as the levels of ATP decline with age or mitochondrial impairment, this could lead to increased aggregation and consequently neurodegenerative decline during aging. Our work in this paper has focused on the role of ATP in keeping unstructured proteins soluble, because these are the types of proteins that have a propensity to form pathological aggregates (*35*). It will be interesting to examine the role of high ATP concentrations in stability and function of multimolecular protein machines.

More generally, during evolution, the production of complex macromolecules would have immediately presented the problem of aggregation. As one of the basic building blocks in RNA and DNA, ATP may have been coopted early in evolution to prevent such aggregation. It is ideal for this purpose, due to the high activation energy required to hydrolyze the polyphosphate bonds in an ATP-Mg-water complex. ATP could later have been adopted to provide the basic energy source for metabolism, which is the hydrolysis of ATP to ADP.

REFERENCES AND NOTES

1. C. P. Brangwynne, T. J. Mitchison, A. A. Hyman, *Proc. Natl. Acad. Sci. U.S.A.* **108**, 4334–4339 (2011).
2. S. Jain *et al.*, *Cell* **164**, 487–498 (2016).
3. A. A. Hyman, C. A. Weber, F. Jülicher, *Annu. Rev. Cell Dev. Biol.* **30**, 39–58 (2014).
4. M. Polymenidou *et al.*, *Brain Res.* **1462**, 3–15 (2012).
5. W. Y. Wang *et al.*, *Nat. Neurosci.* **16**, 1383–1391 (2013).
6. X. Wang *et al.*, *Nature* **454**, 126–130 (2008).
7. A. Patel *et al.*, *Cell* **162**, 1066–1077 (2015).
8. K. A. Burke, A. M. Janke, C. L. Rhine, N. L. Fawzi, *Mol. Cell* **60**, 231–241 (2015).
9. T. W. Traut, *Mol. Cell. Biochem.* **140**, 1–22 (1994).
10. K. Clarke *et al.*, *J. Biol. Chem.* **271**, 21142–21150 (1996).
11. S. Saha *et al.*, *Cell* **166**, 1572–1584 (2016).
12. T. J. Nott *et al.*, *Mol. Cell* **57**, 936–947 (2015).
13. P. Debye, E. Hückel, *Phys. Z.* **24**, 185–206 (1923).
14. E. Gout, F. Rébeillé, R. Douce, R. Bligny, *Proc. Natl. Acad. Sci. U.S.A.* **111**, E4560–E4567 (2014).
15. D. Balasubramanian, V. Srinivas, V. G. Gaikar, M. M. Sharma, *J. Phys. Chem.* **93**, 3865–3870 (1989).
16. C. Neuberg, *Biochem. Z.* **76**, 107–176 (1916).
17. J. Eastoe, M. H. Hatzopoulos, P. J. Dowding, *Soft Matter* **7**, 5917–5925 (2011).
18. C. V. Subbarao, I. P. K. Chakravarthy, A. V. S. L. Sai Bharadwaj, K. M. M. K. Prasad, *Chem. Eng. Technol.* **35**, 225–237 (2012).
19. J. J. Booth, S. Abbott, S. Shimizu, *J. Phys. Chem. B* **116**, 14915–14921 (2012).
20. J. J. Booth, M. Omar, S. Abbott, S. Shimizu, *Phys. Chem. Chem. Phys.* **17**, 8028–8037 (2015).
21. S. Shimizu, N. Matubayasi, *J. Phys. Chem. B* **118**, 10515–10524 (2014).
22. V. Srinivas, D. Balasubramanian, *Langmuir* **14**, 6658–6661 (1998).
23. D. W. Bolen, I. V. Baskakov, *J. Mol. Biol.* **310**, 955–963 (2001).
24. P. H. Yancey, M. E. Clark, S. C. Hand, R. D. Bowlus, G. N. Somero, *Science* **217**, 1214–1222 (1982).
25. G. G. Glenner, C. W. Wong, *Biochem. Biophys. Res. Commun.* **120**, 885–890 (1984).
26. R. Halfmann *et al.*, *Nature* **482**, 363–368 (2012).
27. S. N. Timasheff, *Biochemistry* **41**, 13473–13482 (2002).
28. S. Shimizu, N. Matubayasi, *J. Phys. Chem. B* **118**, 3922–3930 (2014).
29. S. Shimizu, D. J. Smith, *J. Chem. Phys.* **121**, 1148–1154 (2004).
30. S. Shimizu, *Proc. Natl. Acad. Sci. U.S.A.* **101**, 1195–1199 (2004).
31. R. Milo, *BioEssays* **35**, 1050–1055 (2013).
32. B. J. Zeskind *et al.*, *Nat. Methods* **4**, 567–569 (2007).
33. S. B. Zimmerman, S. O. Trach, *J. Mol. Biol.* **222**, 599–620 (1991).
34. B. R. Parry *et al.*, *Cell* **156**, 183–194 (2014).
35. S. Alberti, A. A. Hyman, *BioEssays* **38**, 959–968 (2016).

ACKNOWLEDGMENTS

We particularly thank W. Kunz and colleagues for their help, support, advice, and discussions during the preparation of the manuscript. We thank D. Drechsel, A. Nadler, K. Sandhoff, D. Tang, and members of the Hyman, Krishnan, and Alberti laboratories for helpful discussions; B. Bogdanovo and R. Lemaitre for help with protein expression and purification; B. Lombardot and R. Hasse from the Scientific Computing facility for image analysis; and B. Nitzsche and B. Schroth-Diez for help with light microscopy. We gratefully acknowledge funding from the Alexander von Humboldt Foundation (GRO/1156614 STP-2 to A.P. and USA/1153678 STP to S.S.), EMBO ALTF (608-2013 to S.S.), and German Federal Ministry of Research and Education (BMBF 031A359A Max Syn Bio). Y.K. acknowledges the Scientific Innovation Award from the Brain Research Foundation (BRF SIA-2016-01) and start-up funds from the University of Chicago. A.A.H. and A.P. are inventors on patent application 1305-5403-MSG-ZE, submitted by the Max Planck Society, which covers nucleotides as hydrotropes.

SUPPLEMENTARY MATERIALS

www.sciencemag.org/content/356/6339/753/suppl/DC1
Materials and Methods
Supplementary Text
Figs. S1 to S4
Table S1
Movie S1
References (*36*–*41*)

14 March 2016; accepted 24 March 2017
10.1126/science.aaf6846